Annual Review of Marine Science

Global Quaternary Carbonate Burial: Proxy- and Model-Based Reconstructions and Persisting Uncertainties

Madison Wood,[1] Christopher T. Hayes,[2] and Adina Paytan[3]

[1]Department of Earth and Planetary Sciences, University of California, Santa Cruz, California, USA; email: mamwood@ucsc.edu

[2]School of Ocean Science and Engineering, University of Southern Mississippi, Stennis Space Center, Mississippi, USA; email: christopher.t.hayes@usm.edu

[3]Institute of Marine Sciences, University of California, Santa Cruz, California, USA; email: apaytan@ucsc.edu

Annu. Rev. Mar. Sci. 2023. 15:1.1–1.26

The *Annual Review of Marine Science* is online at marine.annualreviews.org

https://doi.org/10.1146/annurev-marine-031122-031137

Keywords

marine carbonate, glacial, interglacial, carbon cycle

Abstract

Constraining rates of marine carbonate burial through geologic time is critical for interpreting reconstructed changes in ocean chemistry and understanding feedbacks and interactions between Earth's carbon cycle and climate. The Quaternary Period (the past 2.6 million years) is of particular interest due to dramatic variations in sea level that periodically exposed and flooded areas of carbonate accumulation on the continental shelf, likely impacting the global carbonate budget and atmospheric carbon dioxide. These important effects remain poorly quantified. Here, we summarize the importance of carbonate burial in the ocean–climate system, review methods for quantifying carbonate burial across depositional environments, discuss advances in reconstructing Quaternary carbonate burial over the past three decades, and identify gaps and challenges in reconciling the existing records. Emerging paleoceanographic proxies such as the stable strontium and calcium isotope systems, as well as innovative modeling approaches, are highlighted as new opportunities to produce continuous records of global carbonate burial.

1. INTRODUCTION

Carbonate production: precipitation of biogenic carbonate by shallow marine and pelagic calcifiers (e.g., corals, coccolithophores, and foraminifera)

Carbonate accumulation: vertical export of carbonate to the seafloor plus reef production and imported sediment, less dissolution and lateral transport; also referred to as carbonate burial

Carbonate compensation depth (CCD): the depth at which carbonate export from the surface ocean is equal to carbonate dissolution, such that no carbonate is preserved below this depth

Carbonate preservation: the difference between carbonate export and dissolution in the water column or sediments, which ultimately determines how much carbonate is buried

Lysocline: the depth at which carbonate dissolution rapidly increases as a function of the carbonate ion concentration in seawater

Marine carbonate burial is an important component of the global carbon cycle, with large quantities of carbonate stored in ocean sediments ($\sim 5 \times 10^3$ Gt C) and the lithosphere ($\sim 7 \times 10^7$ Gt C) (Zeebe 2012). The carbonate flux influences atmospheric and oceanic inventories of carbon on 1,000- to 100,000-year timescales, playing a potentially important role in glacial/interglacial climate transitions during the Quaternary Period (the past 2.6 My) (Zeebe 2012). Indeed, carbonate deposition has often been invoked to explain changes in Quaternary ocean chemistry and atmospheric carbon dioxide (CO_2) concentrations (e.g., Berger 1982, Brovkin et al. 2007, Kerr et al. 2017, Kohfeld & Ridgwell 2009, Opdyke & Walker 1992, Rickaby et al. 2010, Ridgwell et al. 2003, Vecsei & Berger 2004, Walker & Opdyke 1995). However, robust quantitative constraints on global Quaternary carbonate burial remain elusive.

The last comprehensive review of carbonate production and accumulation over the past ~20 ky (Milliman 1993) provided flux estimates across neritic environments (coral reefs, banks, bays, and continental shelves) and pelagic environments [slopes, enclosed basins, and the deep sea above the carbonate compensation depth (CCD)] (**Table 1**). Many of these estimates had uncertainties of ≥100% (Iglesias-Rodriguez et al. 2002, Milliman & Droxler 1996) due to the scarcity of deep-sea (pelagic) records and lack of knowledge about carbonate accumulation and preservation in shallow (neritic) marine settings. These gaps motivated further study of Quaternary carbonate fluxes over the following decades.

This review incorporates updated proxy- and model-based estimates of global Quaternary carbonate burial and summarizes progress since the review by Milliman (1993). In the following sections, we summarize the importance of carbonate burial in the modern and Quaternary ocean (Sections 1.1–1.3) and review the methods commonly used to reconstruct past carbonate burial fluxes in pelagic (Section 2) and neritic (Section 3) environments. We then evaluate new estimates of global carbonate burial over the Quaternary (Section 4) and suggest areas for further work that may address ongoing challenges (Section 5).

1.1. The Long-Term Carbon Cycle

Carbonate burial is a key flux in the global carbon cycle (**Figure 1**), which has been described in several books, reviews, and publications (e.g., Archer 2010; Berner 2003, 2004; Isson et al. 2020; Sundquist & Visser 2003; Wallmann & Aloisi 2012). Here, we provide a brief carbonate-centered summary (Andersson 2014; Broecker 2003, 2009).

Dissolved calcium (Ca^{2+}) and bicarbonate (HCO_3^-) in seawater are supplied by continental weathering and utilized by organisms (e.g., foraminifera, coccolithophores, and corals) to form calcium carbonate ($CaCO_3$) shells and skeletons. The three most abundant carbonate minerals in marine sediments are (in order of increasing solubility) calcite, aragonite, and high-magnesium calcite (Andersson 2014). In general, $CaCO_3$ solubility increases with depth, and dissolution becomes thermodynamically favorable at the saturation horizon, below which lies the lysocline (the depth at which dissolution increases dramatically). The CCD defines the depth where $CaCO_3$ supply is balanced by dissolution and below which no $CaCO_3$ is preserved (**Figure 1**). Where the seafloor lies above the CCD, a fraction of the $CaCO_3$ produced in the ocean is preserved in sediments. Over millions of years, the sequestered carbon is returned to the atmosphere via subduction and volcanism (**Figure 1**). The effects of carbonate burial on ocean chemistry and atmospheric CO_2 (see the sidebar titled Effect of Carbonate Burial on Ocean Carbonate Chemistry and Atmospheric CO_2) have been thoroughly discussed by Ridgwell & Zeebe (2005) and Zeebe (2012).

Table 1 Updated global estimates of modern $CaCO_3$ production and accumulation rates across depositional environments

Environment	$CaCO_3$ production (Gt y^{-1})	$CaCO_3$ accumulation (Gt y^{-1})	Reference
Coral reefs	0.9	0.7	Milliman 1993
	0.9–1.68	NA	Kleypas 1997
	1.3	NA	Ryan et al. 2001
	0.9	0.7	Iglesias-Rodriguez et al. 2002
	0.65–0.83	NA	Vecsei 2004b
	1.6[a]	1.3[a]	Smith & Mackenzie 2016
	NA	0.7	O'Mara & Dunne 2019
	NA	1.1[b]	Hinestrosa et al. 2022
Banks/bays	0.4	0.2	Milliman 1993
	0.4	0.2	Iglesias-Rodriguez et al. 2002
	0.2	0.1	Smith & Mackenzie 2016
	NA	0.36	O'Mara & Dunne 2019
Carbonate shelves	0.75	0.45	Milliman 1993
	0.37–1.17	0.47	Iglesias-Rodriguez et al. 2002
	2.4[c]	0.7[c]	Smith & Mackenzie 2016
	NA	0.31	O'Mara & Dunne 2019
Noncarbonate shelves	0.4	0.1	Milliman 1993
	0.4	0.1	Iglesias-Rodriguez et al. 2002
	NA	0.002	O'Mara & Dunne 2019
Slopes[d]	0.83	0.58	Milliman 1993
	0.85	0.6	Milliman & Droxler 1996
	0.83	0.57	Iglesias-Rodriguez et al. 2002
Basins	0.03	0.1	Milliman 1993
Deep sea	2.4[e]	1.1	Milliman 1993
	NA	0.86	Catubig et al. 1998
	NA	1.08	Dunne et al. 2012
	13.3	1.1	Smith & Mackenzie 2016
	NA	1.14	Cartapanis et al. 2018 (sediment data)
	NA	1.05	Cartapanis et al. 2018 (metamodel)
	NA	1.13	Hayes et al. 2021

Abbreviation: NA, not applicable.
[a]Explicitly includes visible and submerged reef areas.
[b]Reef accumulation plus contribution from *Halimeda* bioherms for 8–0 ka.
[c]Total shelf production and accumulation, including tropical and extratropical shelves, as defined by Smith & Mackenzie (2016).
[d]Includes imported carbonate flux.
[e]Flux at approximately 1,000-m water depth.

1.2. Overview of Modern Carbonate Production and Burial

Carbonate accumulation depends on production by benthic and planktonic organisms, export from the surface ocean to depth, and preservation on the seafloor (**Figure 2**). Relatively more aragonite and high-magnesium calcite are produced in neritic environments by organisms such as corals, algae, and echinoderms compared with the deep ocean, where calcite is the dominant phase (Andersson 2014). In the modern ocean, pelagic carbonate accumulation varies by region and seafloor depth, with higher rates in the Atlantic, eastern equatorial Pacific, and Indian Oceans,

Carbonate export: the flux of biogenic carbonate from the surface ocean to the deep sea or seafloor

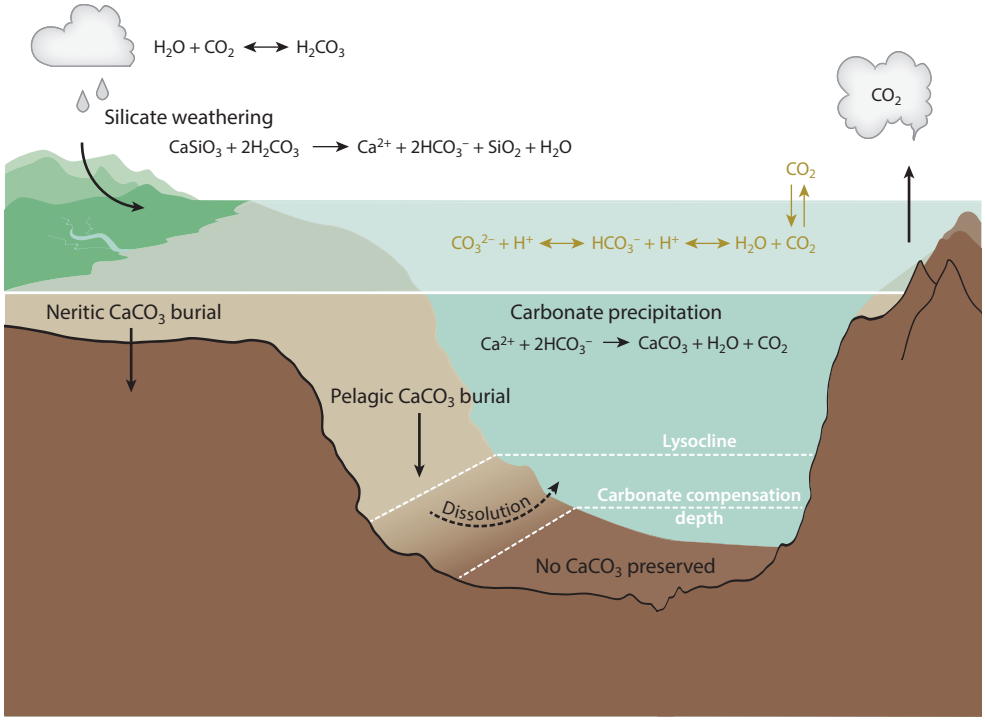

Figure 1

The long-term carbon cycle and ocean carbonate chemistry. Silicate weathering and the sequestration of carbon in carbonate sediments balance volcanic release of CO_2 to the atmosphere on million-year timescales (*black arrows*). Carbonate equilibria between species of dissolved inorganic carbon in seawater (*yellow arrows*) regulate seawater pH, the precipitation and dissolution of $CaCO_3$, and atmospheric CO_2.

EFFECT OF CARBONATE BURIAL ON OCEAN CARBONATE CHEMISTRY AND ATMOSPHERIC CO_2

Carbonate burial is linked to atmospheric CO_2 by the equilibria of ocean carbonate chemistry (**Figure 1**). In seawater, gaseous CO_2 reacts with water to form carbonic acid (H_2CO_3), which subsequently dissociates into bicarbonate (HCO_3^-) and carbonate (CO_3^{2-}) ions. The sum of these dissolved species is called dissolved inorganic carbon (DIC) (equal to $[HCO_3^-] + [CO_3^{2-}] + [CO_2]$). Total alkalinity (TA) describes the excess of proton acceptors (which provide buffering capacity against acidification) over proton donors in seawater, often expressed as carbonate alkalinity or $[HCO_3^-] + 2[CO_3^{2-}]$, although the strict definition of TA includes additional proton acceptors [$B(OH)_4^-$, OH^-, $H_3SiO_4^-$, etc.].

The precipitation of $CaCO_3$ lowers DIC and TA by consuming HCO_3^-, counterintuitively increasing pCO_2. The dissolution of $CaCO_3$ in the deep ocean increases DIC and TA. Carbonate compensation maintains a balance between the input of TA from continental weathering and removal of TA by carbonate burial, so that an increase (decrease) in weathering inputs is balanced by a deepening (shoaling) of the CCD and increase (decrease) in carbonate burial (Broecker & Peng 1982, 1987; Zeebe & Westbroek 2003). On glacial/interglacial timescales, temporary imbalances caused by reduced carbonate accumulation in the shallow ocean due to sea level regression potentially contributed to changing atmospheric pCO_2 (Berger 1982, Opdyke & Walker 1992, Ridgwell et al. 2003, Walker & Opdyke 1995).

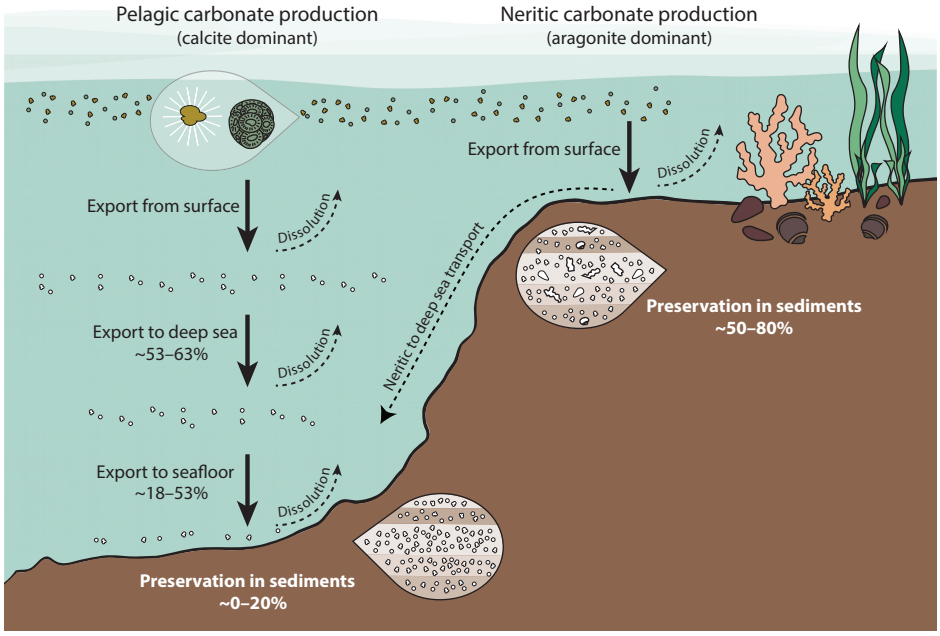

Figure 2

Marine carbonate fluxes in neritic (shallow ocean) and pelagic (open ocean) environments. Pelagic carbonate is produced in the surface ocean and exported down through the water column, where ~47–82% is dissolved before reaching the sediments (Battaglia et al. 2016, Sulpis et al. 2021). An estimated 37–47% of the surface export flux dissolves in the upper water column (<1,500-m depth) (Battaglia et al. 2016, Sulpis et al. 2021), with up to ~44% dissolution below 1,500 m (Battaglia et al. 2016). Approximately 18–53% of the surface flux makes it to the seafloor, where further dissolution reduces the proportion of buried carbonate to ~0–20%. Carbonate preservation is higher in neritic environments, where ~50–80% of the carbonate accumulated by benthic organisms and exported from surfaces waters is preserved (Milliman 1993, Smith & Mackenzie 2016). A substantial fraction of neritic carbonate may be transported from shelves and platforms to the deep sea by nepheloid plumes and gravity flows (e.g., see Jorry et al. 2020).

where the CCD is deeper, and very little accumulation in the North Pacific and Southern Oceans (Dunne et al. 2012, Hayes et al. 2021) (**Figure 3*b***). Key regions of shallow carbonate accumulation are the western Pacific Ocean, eastern Indian Ocean, and Caribbean Sea (O'Mara & Dunne 2019).

Present-day global carbonate accumulation has been quantified by various approaches, including sediment trap data, core-top measurements, and numerical modeling (e.g., Catubig et al. 1998, Iglesias-Rodriguez et al. 2002, Kleypas 1997, Milliman 1993). Global estimates typically rely on site-specific measurements that are interpolated under a set of assumptions (e.g., average production rates across regions, spatial extent of deposition environments, and degree of preservation). Consequently, these global estimates have large uncertainties, particularly in shallow marine environments, where we have little information about export and preservation. Transport of neritic sediments to the deep sea has been well documented, particularly for sea level highstands (Schlager et al. 1994), but quantitative models are necessary to account for this flux in global carbonate budgets. A recent study of an isolated carbonate platform in the Indian Ocean suggested that approximately half of the Holocene $CaCO_3$ production on the platform was transported downslope to the deep basin (Jorry et al. 2020). Further investigation of other regions and neritic settings will be useful for refining this first estimate.

Pelagic carbonate: carbonate produced in the open ocean away from the coast (oceanic zone, >200-m depth); also known as deep-sea carbonate

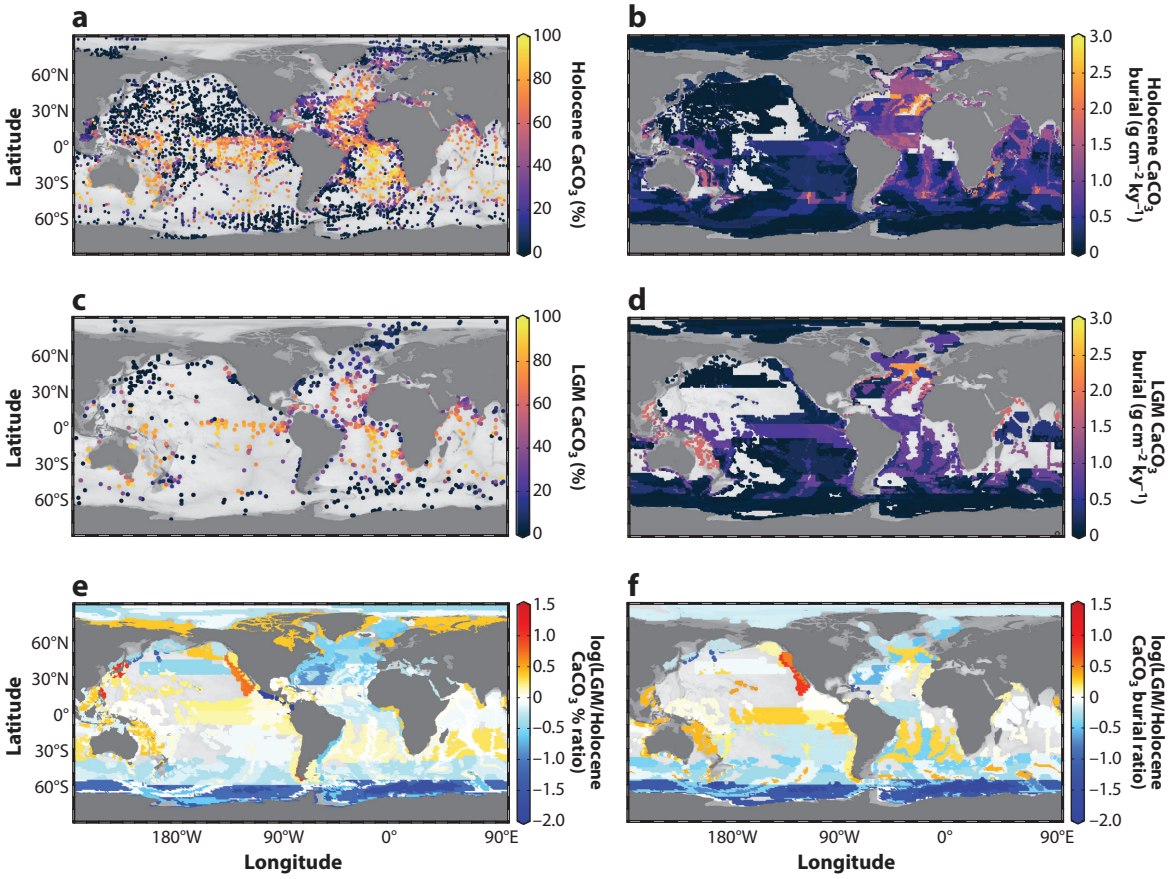

Figure 3

(*Top*) Holocene (0–10 ka) marine sediment $CaCO_3$ content (panel *a*) and burial flux (panel *b*). The Holocene $CaCO_3$ content is a compilation of approximately 7,800 direct observations. The burial estimates are made only for water depths greater than 1 km and are based on ^{230}Th-normalized flux observations (Costa et al. 2020) combined with the sediment composition data. Burial fluxes are interpolated within 254 zones based on Longhurst biogeochemical provinces and water depth. Gray zones indicate areas where no data are available. (*Middle*) LGM (18.5–23.5 ka) distribution of marine sediment $CaCO_3$ content (panel *c*) and burial flux interpolated across biogeochemical province and depth zones as described by Hayes et al. (2021) (panel *d*) using an LGM compilation of ^{230}Th-normalized fluxes (Costa et al. 2020) and an updated $CaCO_3$ content database for the LGM presented here. (*Bottom*) The logarithmic ratios of the LGM $CaCO_3$ content (panel *e*) and burial flux (panel *f*) compared with those of the Holocene (panels *a* and *b*; Hayes et al. 2021). Abbreviation: LGM, Last Glacial Maximum. Panels *a* and *b* adapted with permission from Hayes et al. (2021) (CC BY-NC 4.0).

Pelagic carbonate accumulation is well constrained and constitutes approximately half of the carbonate budget (**Table 1**). Though pelagic carbonate production is significantly lower than shallow-water production, the pelagic area ($\sim 300 \times 10^6$ km^2) is much larger than other depositional areas (Milliman 1993). Hayes et al. (2021) recently calculated a Holocene pelagic burial flux of 1.13 ± 0.28 Gt $CaCO_3$ y^{-1}, leveraging a new database of ^{230}Th-normalized sediment fluxes (Costa et al. 2020) with existing sediment composition data. This estimate agrees with the previously estimated range of 0.83–1.25 Gt $CaCO_3$ y^{-1} (Cartapanis et al. 2018).

Sparse observations and poorly constrained preservation and export rates have limited estimates of carbonate accumulation in shallow marine environments (Iglesias-Rodriguez et al. 2002, O'Mara & Dunne 2019). The latest estimates utilize new data, including bathymetric maps and

$CaCO_3$ fluxes derived from satellite data, with improved mapping of neritic community types (O'Mara & Dunne 2019). Uncertainties associated with burial on carbonate-rich shelves (±39%) and bays (±46%) (O'Mara & Dunne 2019) were substantially lower than those previously reported (>100% for carbonate-rich shelves, ±100% for bays) (Iglesias-Rodriguez et al. 2002). The uncertainty for carbonate-poor shelf burial (±178%) remains high (O'Mara & Dunne 2019).

1.3. Overview of Quaternary Carbonate Burial

Quaternary carbonate burial varied over glacial/interglacial cycles due to differences in biological production, ocean circulation, deep-sea sequestration of respired CO_2, and sea level fluctuations (e.g., deMenocal et al. 1997, Hain et al. 2014, Jaccard et al. 2009, Kleypas 1997) (**Figure 4**). The dominant location of carbonate deposition likely shifted from shallow- to deep-water environments during glacial stages due to a reduction in the submerged area of continental shelves, carbonate platforms, and atolls (Berger 1982, Opdyke & Walker 1992). Models and observations suggest that while modern carbonate burial rates in neritic and pelagic environments are

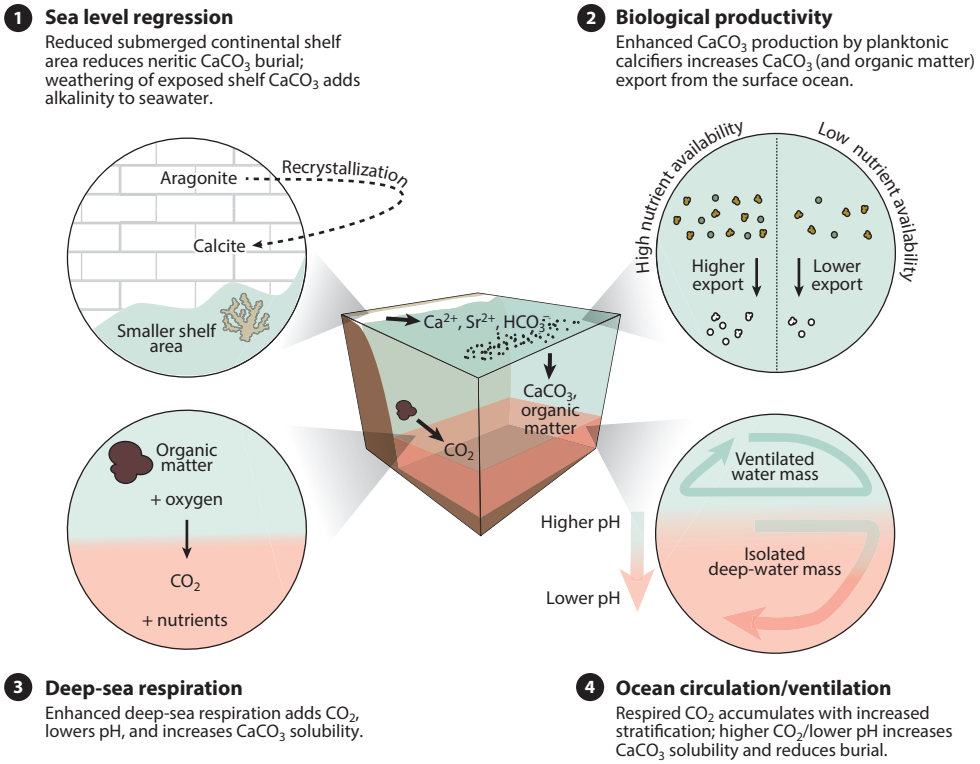

Figure 4

Processes hypothesized to alter carbonate burial rates over glacial/interglacial cycles, by changing the carbonate equilibria of the ocean (via inputs of alkalinity or dissolved inorganic carbon), production of biogenic carbonate in the surface ocean, and/or physical area available for carbonate burial (on continental shelves and above the carbonate compensation depth). These processes do not necessarily act in isolation; rather, feedbacks between processes may enhance or balance the effect of others. For example, ocean circulation changes may isolate the deep ocean from the surface, causing the accumulation of respired carbon and limiting mixing of nutrients back to the surface ocean for utilization by calcifiers.

Neritic carbonate: carbonate produced in coastal or shallow marine environments above the continental shelf break (<200-m depth)

approximately equal (Milliman 1993), neritic burial rates would have been lower due to reduced glacial shelf area (Kleypas 1997).

The coral reef hypothesis (Berger 1982, Opdyke & Walker 1992, Ridgwell et al. 2003, Vecsei & Berger 2004, Walker & Opdyke 1995) proposed that sea level–driven changes in neritic carbonate burial impacted atmospheric CO_2 concentrations (pCO_2) over the Quaternary. Assuming constant alkalinity input from continental weathering, reduced neritic carbonate burial during glacial periods would increase whole-ocean alkalinity and consequently reduce pCO_2. For the carbonate budget to maintain steady state, increased deep-sea burial must restore the alkalinity balance and stabilize pCO_2 (Sigman & Boyle 2000). Counterarguments to the coral reef hypothesis have cited lack of evidence for a glacial increase in global deep-sea burial (Archer & Maier-Reimer 1994, Sigman & Boyle 2000, Zeebe & Marchitto 2010). However, the Quaternary carbonate budget may have operated in a nonsteady state imposed by sea level fluctuations (Milliman & Droxler 1996). Similarly, on short timescales, the assumption of constant alkalinity input may not be maintained due to changes in weathering regimes and weatherability following glacial retreats (Vance et al. 2009). The question of steady state versus nonsteady state is unanswered but may be resolved as global carbonate burial estimates for glacial/interglacial cycles improve. In Section 4, we discuss significant advances toward continuous records of Quaternary carbonate burial, including efforts to model variations in reef productivity since 1,500 ka (Husson et al. 2018) and updated compilations of deep-sea sedimentary records that constrain global pelagic burial during the Holocene, the Last Glacial Maximum (LGM), and continuously over the last 150 ky (Cartapanis et al. 2018, Hayes et al. 2021, this review).

2. METHODS FOR RECONSTRUCTING DEEP-SEA CARBONATE BURIAL

The marine sedimentary record provides information about pelagic carbonate burial, which varies in space and time due to depth (solubility), regional productivity, lateral transport, CCD position, and dissolution in sediments (Dunne et al. 2012). While past changes in carbonate burial were observed early on in pelagic sediments in the Pacific, Atlantic, and Indian Oceans (e.g., Archer 1991, Arrhenius 1952, Balsam & McCoy 1987, Biscaye et al. 1976, Milliman 1993), initial reconstructions of pelagic carbonate burial were limited by poor core chronology and sparse observations (Van Andel et al. 1975). Furthermore, while carbonate accumulation records can be obtained from deep-sea sediment cores with relative ease, drilling on slopes is technically difficult, and few $CaCO_3$ accumulation records exist for these environments. Methods for obtaining globally integrated estimates of the pelagic carbonate burial flux from deep-sea sediment cores are summarized below.

2.1. Calcium Carbonate Weight Percent

$CaCO_3$ content in sediment cores is widely used to infer changes in carbonate burial through time. $CaCO_3$ wt% is measured using a variety of analytical methods, most commonly coulometry and loss on ignition (Fu et al. 2020, Kastens et al. 1987, Mörth & Backman 2011). High-resolution scans of physical properties (e.g., bulk density and reflectance spectra) have also been used to determine sediment carbonate content (Vanden Berg & Jarrard 2002, 2006, and references therein). Despite the relative ease of measuring sediment carbonate content, $CaCO_3$ wt% alone cannot be used to determine accumulation or burial rates because it is a proportional unit and depends on the content of other sedimentary fractions. For the same flux of carbonate delivered to the seafloor, $CaCO_3$ wt% can vary significantly due to dilution by noncarbonate minerals and/or postdepositional dissolution. Comparison of carbonate content between regions is also

complicated by spatial variability in dilution and dissolution that may bias $CaCO_3$ wt% values. Consequently, $CaCO_3$ wt% should be converted to a mass flux using a bulk sedimentation rate.

Calcium carbonate saturation state: the product of $[Ca^{2+}]$ and $[CO_3^{2-}]$ in seawater divided by the solubility product for aragonite or calcite; the saturation state determines the solubility of carbonate in seawater

2.2. Carbonate Mass Accumulation Rates

Records of $CaCO_3$ wt% are converted to carbonate mass accumulation rates (MARs; g cm^{-2} ky^{-1}) by

$$\text{MAR} = \left(\frac{\text{CaCO}_3 \text{ wt\%}}{100}\right)(\rho_{\text{dry}})(S), \quad 1.$$

where ρ_{dry} is the dry bulk density (g cm^{-3}) and S is the linear or instantaneous sedimentation rate (cm ky^{-1}). Age model–derived (linear) sedimentation rates have traditionally been used but may be biased by redistribution of sediments on the seafloor (Costa et al. 2020, Francois et al. 2004). Constant flux proxies such as excess ^{230}Th and ^{3}He are now used to derive instantaneous sedimentation rates and can correct for sediment redistribution (e.g.,^{230}Th normalization) (Costa et al. 2020, Francois et al. 2004, McGee et al. 2010). Age model–derived sedimentation rates capture average vertical sedimentation and lateral advection between sampling horizons; instantaneous sedimentation rates reflect only vertical sedimentation (McGee et al. 2010). In most regions of the ocean, constant flux proxies are the preferred method for calculating carbonate (and other sedimentary component) MARs (Costa et al. 2020).

Milliman (1993) reviewed studies of carbonate MARs made possible by age models based on oxygen isotopes and radiocarbon dating that were published before 1993. In the years since 1993, carbonate MARs have been reported in numerous studies and locations in the ocean, some derived from constant flux proxies (Section 4.1). Global estimates of deep-sea carbonate burial from MARs require nontrivial compilations of globally extensive MAR records and interpolation between site-specific records to resolve spatial variability (Cartapanis et al. 2018, Catubig et al. 1998, Hayes et al. 2021).

2.3. Carbonate Compensation Depth

Reconstructions of the CCD, which reflects the ocean calcium carbonate saturation state (Ridgwell & Zeebe 2005), are also used to constrain pelagic carbonate burial. The CCD is operationally defined by the depth of a specific sedimentary $CaCO_3$ wt% (e.g., 20%; Van Andel 1975) or the depth at which carbonate accumulation rates approach zero (Lyle 2003). Although the position of the CCD is relatively easy to identify with sediment cores, linking changes in the CCD to carbonate burial can be challenging due to potential decoupling between carbonate burial and the CCD response. The recent approach of Boudreau & Luo (2017), who modeled global pelagic carbonate burial based on the Cenozoic CCD, is relevant only to secular timescales (>0.5 Ma, not applicable to glacial/interglacial cycles). In general, extrapolating CCD reconstructions from a particular ocean basin to a global CCD record is complicated by ocean circulation, which could shift the CCD regionally (Greene et al. 2019). Furthermore, burial of excess $CaCO_3$ above the CCD could cause a decoupling of the CCD and global carbonate burial (Greene et al. 2019) such that changes in ocean alkalinity are accommodated by increased burial above a relatively stable CCD.

During the Quaternary, the Pacific CCD appears to have remained relatively stable despite large sea level fluctuations (Farrell & Prell 1989, Lyle 2003, Lyle et al. 2008, Pälike et al. 2012). The lack of significant CCD change during glacial/interglacial cycles may be explained by reduced sensitivity of the Cenozoic CCD to shifts in shelf carbonate burial following the CCD deepening and reduction of shelf carbonate globally at the Eocene–Oligocene transition (~34 Ma)

(Armstrong McKay 2015). In this case, shifts in shelf–basin partitioning of carbonate burial in response to glacial/interglacial sea level change (or other mechanisms of alkalinity transfer) may not be evident in Quaternary CCD records but rather reflected in changes in the carbonate accumulation between the lysocline and the CCD, which is much harder to assess. Regional shifts in the lysocline can be inferred from observed carbonate dissolution cycles on glacial/interglacial timescales. Anticorrelated Pacific–Atlantic preservation cycles are well documented for the Pleistocene (e.g., Farrell & Prell 1989), and carbonate dissolution cycles similar to those in the Pacific have been observed throughout the Indian Ocean (Bassinot et al. 1994). In general, preservation of carbonate in the Pacific and Indian Oceans is enhanced during glacial periods, while sediments in the Atlantic experience increased dissolution; the reverse is true during interglacial periods. Though carbonate preservation and dissolution are clearly linked to glacial/interglacial cycles, the challenge is to determine whether opposing changes in different ocean basins maintained a relatively constant global pelagic $CaCO_3$ accumulation rate or were imbalanced such that a net change in global carbonate burial occurred.

3. METHODS FOR RECONSTRUCTING NERITIC CARBONATE BURIAL

The heterogeneous nature of carbonate production across neritic environments is a significant challenge to global reconstructions because they require extrapolation of locally reconstructed production (or burial) rates. Furthermore, since carbonate production in these environments is especially sensitive to sea level fluctuations, nutrient levels, temperature, and salinity, production (and burial) rates may vary through time depending on environmental conditions. Variable preservation, erosion, and transport of neritic sediments further complicate carbonate burial estimates in this zone. Below, we highlight approaches that have been used to investigate changes in neritic carbonate burial through time as well as their limitations.

3.1. Fossil Coral Reefs

Coral reefs constitute a substantial fraction of global carbonate production and accumulation, yet quantifying this contribution remains challenging because observation-based estimates are often region or reef specific. Methods for observing reef production include hydrochemistry, census data, accumulated sediments, and numerical modeling; Vecsei (2004b) provided a detailed review of these methods and previous estimates, including modeling by Kleypas (1997). These approaches often suffer from insufficient data and large uncertainties that are magnified when scaling local and regional studies to global estimates. Current reef production estimates for the Holocene range from 0.65 to 1.68 Gt $CaCO_3$ y^{-1} and, as Vecsei (2004b, p. 12) succinctly noted, are "fraught with substantial, unquantified uncertainties." Several reef accumulation estimates agree with Milliman's (1993) early estimate of 0.7 Gt $CaCO_3$ y^{-1}, with uncertainty in the range of 100% (**Table 1**). Importantly, estimates typically exclude carbonate mounds formed by cold-water corals, which have been documented throughout the ocean and may contribute significantly to carbonate budgets but whose accumulation rates are even more poorly quantified than those of tropical reefs (e.g., Hebbeln et al. 2019; Lindberg & Mienert 2005; Titschack et al. 2015, 2016).

Constraining reef production, preservation, and geographic extent becomes increasingly difficult the further back one goes in geologic history. Coral reef accumulation is not constant through time or space and varies with changing sea level. Direct measurements of reef accretion rates through time can be made by radiometric dating of growth stages (e.g., Camoin et al. 2001), but current observations are sparse and limited by diagenesis, lack of dateable material required for U/Th chronology, and absence of lowstand reef units (Camoin & Webster 2015). Without widespread observations, we require an alternative approach for estimating Quaternary reef

carbonate burial prior to the LGM. In Section 4.3, we discuss recent studies that have turned to numerical modeling to simulate reef production and predict global accumulation rates (Husson et al. 2018, Jones et al. 2015).

3.2. Other Carbonate Burial Sinks

Besides corals, the shallow ocean hosts an array of habitats and communities of calcifiers that contribute to the global carbonate budget but are currently underestimated, due largely to spatial heterogeneity. Carbonate production can be locally monitored in the water column (using sediment traps) or on benthic substrates (for example, colonization experiments with calcification accretion units), though these measurements can be biased by horizontal transport of material and may differ from actual burial rates due to postdepositional dissolution in sediments. Extrapolating local studies to global rates requires that the habitat preferences and distributions of species be well estimated, which remains a challenge at present. For example, *Halimeda* algae are thought to be important contributors to carbonate production in the tropics, but the geographic extent of *Halimeda* accumulation is uncertain and very likely underestimated (McNeil et al. 2016, 2020; Rees et al. 2006). Hinestrosa et al. (2022) recently estimated that at least 590 Gt $CaCO_3$ accumulation by *Halimeda* must be added to global Holocene carbonate budgets (compared with Holocene and drowned reef deposits of ∼8,100 Gt and ∼1,500 Gt $CaCO_3$, respectively) based on their regional study of the Great Barrier Reef. Other benthic calcifiers, such as echinoderms, are probably also underestimated (e.g., Lebrato et al. 2010). A combination of habitat-specific carbonate production or accumulation rates and global surveys of habitat extent is needed to compile accurate neritic carbonate budgets.

4. QUATERNARY CARBONATE BURIAL RECONSTRUCTIONS

4.1. Deep-Sea Carbonate Burial

A primary goal for reconstructing pelagic carbonate burial over the Quaternary is to test whether pelagic burial increased during glacial periods. This hypothesis is based on the expectation that neritic carbonate burial was reduced during glacial periods relative to interglacials, when lower sea level reduced the area available for neritic carbonate accumulation (Kleypas 1997) (**Figure 4**). To maintain a steady-state carbonate budget during a glacial period, carbonate compensation would deepen the CCD and increase deep-sea carbonate burial. Thus, LGM pelagic carbonate burial was predicted to exceed the modern rate by up to two times in a steady-state ocean (Catubig et al. 1998).

To test this expectation, Catubig et al. (1998) used a compilation of records mainly from the Pacific and Atlantic Oceans to compare global Holocene and LGM carbonate burial. Their compilation suggested that deep-sea LGM burial rates were higher than those of the Holocene in the Pacific and North Atlantic but lower in the South Atlantic, Indian, and Southern Oceans. Notably, the South Pacific had a higher $CaCO_3$ wt% during the LGM but was excluded from their analyses for lack of MAR data. The study found no significant difference in global deep-sea carbonate burial between the Holocene (0.86 Gt y^{-1}) and LGM (0.92 Gt y^{-1}), challenging the premise that increased pelagic carbonate burial compensated for lower neritic burial during glacial periods and the assumption of a steady-state carbonate budget on these timescales.

As chronostratigraphy improved and drilling programs expanded over the next two decades, carbonate MAR records became more reliable and more numerous (Anderson et al. 2008; Campbell et al. 2018; Lyle 2003; Lyle et al. 2006, 2019; Pälike et al. 2012; Vanden Berg & Jarrard 2004). The first continuous reconstruction of global deep-sea carbonate burial over the last glacial cycle, by Cartapanis et al. (2018), used a compilation of 637 sediment records (**Figure 5**). To

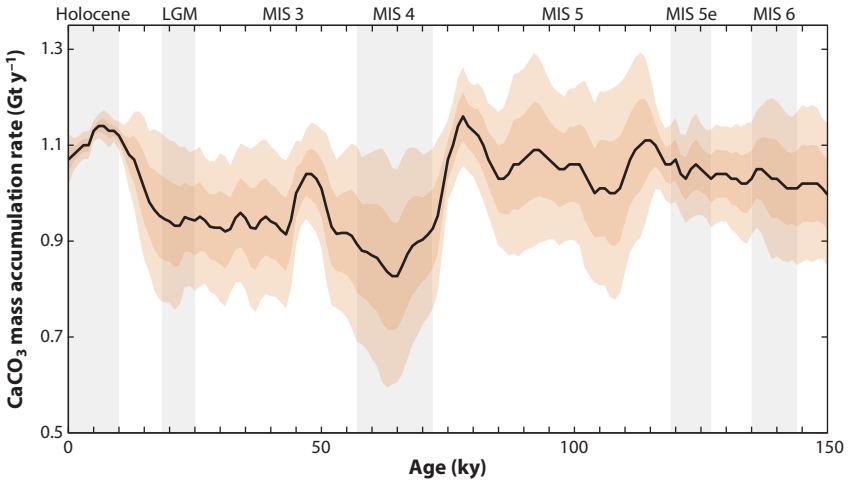

Figure 5

Global deep-sea carbonate mass accumulation rate over the last glacial cycle, as reconstructed by Cartapanis et al. (2018). The black curve shows the mean of 20 scenarios using different biogeochemical province maps, with shaded regions indicating ±1σ and ±2σ. Gray vertical bars delineate glacial (LGM, MIS 4, MIS 6) and interglacial (Holocene, MIS 5e) periods. Abbreviations: LGM, Last Glacial Maximum; MIS, marine isotope stage. Figure adapted from Cartapanis et al. (2018) (CC BY 4.0).

account for the spatial variability of carbonate accumulation, this study identified biogeochemical provinces based on modern carbonate MARs (Dunne et al. 2012) and reconstructed carbonate accumulation in each province over the past 150 ky from available MARs. The global reconstruction showed that carbonate accumulation was similar during the present-day interglacial and marine isotope stage (MIS) 5e, with lower burial during MIS 4 (78% ± 9% of the Holocene value) and MIS 2 (85% ± 7% of the Holocene value); the absolute magnitude of these changes depended on the province map used.

Despite being unable to entirely resolve the challenges of spatial heterogeneity, this reconstruction represented a major step forward, providing a continuous record over an entire glacial cycle and revealing minima during glaciation that could not be resolved by the two-end-member study by Catubig et al. (1998). While both Cartapanis et al. (2018) and Catubig et al. (1998) observed glacial $CaCO_3$ concentrations greater than Holocene values in the Pacific, consistent with the findings of Farrell & Prell (1989), Cartapanis et al. (2018) found that the glacial increase in the Pacific was not sufficient to balance the decrease in the Atlantic. Neither reconstruction supports increased global pelagic carbonate burial during glacial periods; rather, they suggest that pelagic burial did not compensate for the expected decrease in neritic burial.

4.2. Updated ^{230}Th-Normalized Last Glacial Maximum Deep-Sea Carbonate Burial Fluxes

A new database of ^{230}Th-normalized sediment fluxes by Costa et al. (2020) provides an opportunity to revise these estimates for the LGM. As Hayes et al. (2021) did for the Holocene (**Figure 3*a*,*b***), here we newly compile published $CaCO_3$ wt% data for the LGM (**Figure 3*c*,*d***) and combine these composition data with the LGM sediment fluxes (Costa et al. 2020). This allows us to estimate ^{230}Th-normalized $CaCO_3$ burial fluxes for the deep sea at the LGM (defined here as 18.5–23.5 ka) and compare them with those of the Holocene (**Figure 3*e*,*f***).

For the LGM $CaCO_3$ wt% distribution, we utilized previous compilations (Cartapanis et al. 2018, Catubig et al. 1998) and added 95 new observations, for a total database of 898 observations (see the **Supplemental Material**). Reduced $CaCO_3$ content during the LGM compared with the Holocene is seen clearly throughout most of the Atlantic, Southern, and Arctic Oceans. Increased LGM $CaCO_3$ content is seen in the equatorial Pacific and Indian Oceans as well as the Australian, Indonesian, and Arctic shelf seas. However, as mentioned above, these changes in $CaCO_3$ content may not be reflective of actual changes in burial due to variable dilution from other phases and/or changes in the total sedimentation rate.

Our new estimates of LGM carbonate burial are restrained to deep-sea sites (deeper than 1 km), where the assumptions of the ^{230}Th-normalization method are valid (Costa et al. 2020). Additionally, the distribution of ^{230}Th-normalized flux observations for the LGM is sparser than that for the Holocene, resulting in a larger proportion of ocean provinces that cannot currently be characterized. For instance, the Holocene map of ^{230}Th-normalized fluxes covered 87% of the deep-sea area (Hayes et al. 2021), while the areal coverage for the LGM is 49.5%. Nonetheless, sufficient coverage of key regions in the ocean produces results that can help determine LGM carbonate burial changes. With more geographic detail than previously available, we find clear evidence for increased LGM carbonate burial compared with the Holocene in the equatorial Pacific and decreased carbonate burial in most of the North Atlantic and Southern Oceans (**Figure 3*f***). These observations are consistent with the hypothesis that glacial/interglacial carbonate burial variations result mainly from changes in carbonate preservation in the deep ocean, associated with a major change in deep-sea CO_2 storage (e.g., Anderson et al. 2008, Yu et al. 2020). Nonetheless, recent work on modern $CaCO_3$ export fluxes in the water column is revealing previously unrecognized biological production influences on $CaCO_3$ sedimentation, such as the influence of aragonite on calcite preservation (Sulpis et al. 2021, 2022), and there is still much to be discovered about how the LGM calcifier ecosystem was different from today's.

While our interpolated LGM $CaCO_3$ burial map can be used to derive a deep-sea LGM $CaCO_3$ burial sink, some notes on its uncertainty must be mentioned due to its geographic sparseness. We assessed the accuracy of our interpolated LGM $CaCO_3$ burial estimates by comparing predicted $CaCO_3$ burial values with those from the 103 sites where ^{230}Th-normalized $CaCO_3$ fluxes have been observed directly. This analysis results in a root mean square error of 29% of the observed burial flux range. We use this relative root mean square error as our assumed uncertainty in deriving a global LGM $CaCO_3$ burial flux. Furthermore, there is some geographic bias in the areas for which no fluxes can currently be derived, with the lowest coverage in the Indian Ocean (**Figure 3*d***). We therefore used a basin-specific scaling factor to correct for the relative amounts of seafloor missing from the interpolated estimates, aimed at matching the same areal distribution in our Holocene interpolation (**Figure 3*b***) for better comparison.

This process results in a deep-sea LGM burial of 1.3 ± 0.4 Gt $CaCO_3$ y^{-1}, within the error of our Holocene estimate (1.1 ± 0.3 Gt $CaCO_3$ y^{-1}). This analysis adds to the evidence that total deep-sea $CaCO_3$ burial did not change over glacial cycles but makes clear that there were basin-wide fractionations in $CaCO_3$ burial. For instance, the Holocene balance of $CaCO_3$ burial between basins is 40% Atlantic, 22% Pacific, 20% Indian, 17% Southern, and 0.4% Arctic (Hayes et al. 2021; note that in this scheme the Southern Ocean is defined as south of 40°S). By contrast, in our LGM $CaCO_3$ burial reconstruction the balance is 33% Atlantic, 41% Pacific, 17% Indian, 10% Southern, and <0.1% Arctic. This suggests that the increased glacial $CaCO_3$ burial in the Pacific was balanced by reduced carbonate burial in all other basins, rather than only in the Atlantic, as had first been theorized (Balsam 1983, Crowley 1985, Farrell & Prell 1989). More estimates of glacial period ^{230}Th-normalized fluxes from the key gap regions highlighted in **Figure 3*d*** will be necessary to investigate this possibility further.

4.3. Quaternary Coral Reef Accumulation

Fossil coral reefs are important archives of Quaternary sea level change and reef accumulation [see reviews by Dullo (2005) and Camoin & Webster (2015)]. Notable reef sequences used to characterize the last deglaciation include those obtained from Barbados (e.g., Fairbanks 1989), Tahiti (e.g., Camoin et al. 2012), and the Great Barrier Reef (e.g., Webster et al. 2018, Yokoyama et al. 2018), while drilling efforts in regions such as New Caledonia have yielded records extending through earlier glacial stages (e.g., Cabioch et al. 2008, Montaggioni et al. 2011). An exceptional example is the 300-ky record obtained by Camoin et al. (2001), which contains both sea level high- and lowstand reef units, an uncommon achievement in coral reef drilling (Camoin & Webster 2015). More recently, the 30-ky record from the Great Barrier Reef documented reef accretion rates and the presence of shelf-edge reefs during the LGM (Webster et al. 2018, Yokoyama et al. 2018). Such direct observations constrain reef establishment and productivity only for specific locations, so global estimates of reef productivity rely on a limited number of records to be representative of reefs globally (e.g., Hinestrosa et al. 2022, Ryan et al. 2001, Vecsei & Berger 2004).

Based on the recent data from the Great Barrier Reef (Webster et al. 2018, Yokoyama et al. 2018), Hinestrosa et al. (2022) attempted a global estimate of postglacial reef accumulation that accounted for both Holocene reef accumulation and drowned reefs (established on the shelf edge during the LGM). They reported global estimates of ∼1 Gt $CaCO_3$ y^{-1} for Holocene reefs (8–0 ka) and 0.2 Gt $CaCO_3$ y^{-1} for drowned reefs (19–10 ka), noting that the extrapolation from Great Barrier Reef estimates to global estimates strongly depends on the value used for global reef area. In any case, the finding that drowned reefs may equal ∼16–40% of the Holocene reef deposits at the Great Barrier Reef suggests an important role for drowned reefs in the global carbonate budget, and the calculated rate of accumulation for drowned reefs prior to 8 ka is similar to a previous estimate by Vecsei & Berger (2004).

Vecsei & Berger (2004) estimated global reef accumulation since the LGM by combining fossil records from tropical and subtropical reefs and using sea level records and reef depth distributions to identify patterns of reef production. They concluded that reef production during the LGM and initial deglaciation (∼21–14 ka) was low [we note that accretion during the 19-ka meltwater pulse (Clark et al. 2004) may have contributed but is not quantified here], while the late deglaciation (∼10–6 ka) saw the highest production with slowing sea level rise (Vecsei & Berger 2004). Based on an estimate of 80% preservation for reef carbonate (from Milliman 1993) and the extrapolation of modern reef area to past reefs, reef accumulation for 0–6 ka, 6–8 ka, and 8–14 ka was estimated to be 0.23, 0.41, and 0.12 Gt $CaCO_3$ y^{-1}, respectively. Though limited by a range of uncertainties (e.g., past reef area, global extrapolation of production rates and preservation, contribution from fore reefs and temperate shelves, and intermittent productivity), these estimates are conservative and imply at least a threefold increase in reef accumulation from the LGM (<0.12 Gt $CaCO_3$ y^{-1}) to peak deglacial accumulation (0.41 Gt $CaCO_3$ y^{-1}). The cumulative reef accumulation since 14 ka (∼2,900 Gt $CaCO_3$) was estimated to account for 211 Gt of carbon emissions over the same period; adding conservative estimates for accumulation on isolated banks and platforms (∼250 Gt $CaCO_3$) raised the emissions estimate to 225 Gt of carbon released as CO_2 (Vecsei 2004b, Vecsei & Berger 2004). The effect on atmospheric pCO_2 ultimately depended on the emission rate and uptake by the deep ocean or terrestrial biosphere. These findings were broadly supportive of the coral reef hypothesis (Berger 1982, Opdyke & Walker 1992), with increased coral growth (and CO_2 emissions) coinciding with rising sea level and flooding of continental shelves, where reef habitat is prevalent.

The approach of Vecsei & Berger (2004) cannot reliably be applied to periods earlier than the LGM due to the scarcity of preserved reef records. To assess coral reef accumulation over the Pleistocene, continuous accumulation records extending over multiple glacial cycles are needed.

Obtaining such records from direct observations is currently out of reach, yet numerical modeling offers an alternative approach for global reef accumulation reconstructions. Coral calcification rates have been modeled as a function of environmental factors (e.g., water temperature, light, and carbonate saturation state) to predict reef responses to environmental change (Jones et al. 2015; Kleypas 1997; Kleypas et al. 2011; Lough 2008; Silverman et al. 2007, 2009). While these models are geared toward understanding how future environmental change will impact reefs, they also provide a means of estimating reef production for given environmental conditions. For instance, O'Mara & Dunne (2019) utilized the coral productivity models of Kleypas (1997), Lough (2008), and Silverman et al. (2007) in their estimation of modern neritic carbonate burial (Section 1.3).

Over long timescales, reef productivity also depends on sea level oscillations, uplift, subsidence, substrate morphology, and coastal erosion (Husson et al. 2018). Husson et al. (2018) assumed that the physicochemical factors important for local reef production (e.g., temperature, light, and carbonate saturation state) cancel out on a global scale, so that external factors such as uplift, subsidence, and erosion are the primary drivers of global reef productivity during the Quaternary. Their numerical model simulated reef productivity in response to sea level change, uplift, subsidence, and erosion over 1,500 ky, advancing beyond the modeling of individual reef systems (reviewed in Camoin & Webster 2015) by extrapolating globally (Husson et al. 2018). Taking the last glacial period as representative, the model predicted near-zero reef productivity during sea level regression, a gradual increase during deglaciation to peak Early Holocene productivity (~1.9 Gt $CaCO_3$ y^{-1} around 10 ka), and a slight decrease to the Late Holocene. The timing of the late deglacial production peak aligns with prior observations (Vecsei & Berger 2004), and the predicted Late Holocene production rate (~0.8 Gt $CaCO_3$ y^{-1}) agrees well with observation-based modern estimates (**Table 1**). Across the entire simulation, peak production occurred ~5 ky prior to sea level maxima and lasted several thousand years, with typical values from 2.5 to 4.5 Gt $CaCO_3$ y^{-1} for most late deglacial periods and maxima calculated at MIS 11 and MIS 31 (>10 Gt $CaCO_3$ y^{-1}) (Husson et al. 2018). Lowstands were characterized by negligible production rates.

Global reef accumulation rates were not reported by Husson et al. (2018); accurate conversion of production rates to accumulation rates will require better knowledge of the preservation of reef carbonate over the past 1,500 ky. Approximating 80% preservation (Milliman 1993) yields peak deglacial accumulation rates of 1.5 Gt $CaCO_3$ y^{-1} for the Holocene [more than three times greater than the peak estimate of Vecsei & Berger (2004)] and 2.0–3.6 Gt $CaCO_3$ y^{-1} for most deglaciations, with negligible accumulation during the LGM and other glacial lowstands. Based on their productivity estimates, Husson et al. (2018) predicted ~1,400 Gt of carbon released as CO_2 during the last deglaciation (20–7 ka).

4.4. Quaternary Carbonate Burial on Banks, Shelves, and Slopes

Past carbonate burial on banks, continental shelves, and slopes has remained difficult to estimate for a variety of reasons, particularly the significant spatial and temporal heterogeneity in carbonate production and accumulation (Section 3.2). Current observations are insufficient for compiling a globally representative record of Quaternary carbonate burial in these environments, but localized studies offer some insight into their role in the global carbonate budget. For example, Vecsei (2004a) evaluated carbonate production on isolated carbonate banks (0- to ~70-m depth) from 0 to 20 ka and concluded that carbonate production was low during rapid sea level rise from the LGM to ~14 ka, with episodically increasing production after 14 ka and peak production after 6 ka as sea level rise slowed. The study included only banks at low latitudes since the geographic and depth distributions of high-latitude banks are poorly known; this limitation may be addressed in the future with numerical modeling. Recent work by Laugié et al. (2019) extended the modeling of coral reefs discussed in Section 4.3 by developing a model of shallow marine carbonate

factories in the modern ocean as a function of sea surface temperature and salinity, depth, and primary productivity. Their modeling framework demonstrates the potential for deriving geographic distributions of shallow marine carbonates from oceanographic parameters, which could meet the ongoing need for better spatial characterization in the modern and past ocean.

Continental shelf carbonate burial fluxes are highly location specific due to numerous factors that influence production, transport, and preservation (e.g., upwelling nutrients, riverine fluxes, terrigenous sediment accumulation, presence of *Halimeda* algae, latitude, and seasonality). Consequently, local studies provide depositional models only for certain biogeochemical and oceanographic conditions. For instance, a study of Late Quaternary sediments on the Ross Sea shelf provided insight into carbonate accumulation in a high-energy, glaciation, polar shelf environment (Frank et al. 2014). The scarcity and complexity of these local observations hinder our ability to improve upon the approximation of the global continental shelf carbonate flux made by Milliman (1993), which relied on broad assumptions about the geographic area and average composition of shelf sediments.

Where observations are insufficient, modeling can provide some constraints on shallow burial fluxes. Van der Ploeg et al. (2019) used an alkalinity mass balance model to estimate Cenozoic global carbonate burial along continental margins. Though the contributions of each shallow marine setting cannot be distinguished by this approach, the model yields global neritic carbonate burial estimates that integrate the contributions of each environment. This modeling approach could potentially be applied over shorter timescales (e.g., glacial/interglacial cycles) to resolve changes in neritic carbonate burial. Importantly, the alkalinity input from weathering and the pelagic burial flux must be well constrained over the time interval of interest to solve for the neritic carbonate burial flux using the alkalinity mass balance model. Moreover, this modeling approach assumes steady state (mass balance) in alkalinity input and output on the relevant timescales, which may not hold for the short timescales of glacial/interglacial sea level fluctuations.

4.5. Summary

The available Quaternary reconstructions of pelagic carbonate burial do not indicate that global carbonate burial in the deep sea increased during glacial periods, as would be expected if steady state were maintained over glacial cycles. Our updated compilation of ^{230}Th-normalized LGM carbonate burial fluxes provides further evidence that LGM burial rates were the same as those during the Holocene (within error). The MAR-based reconstruction by Cartapanis et al. (2018) suggested burial minima during glacial periods, which would exacerbate the buildup of ocean alkalinity from the dissolution of exposed shelf carbonates. Records derived from fossil coral reefs generally confirm that reef accumulation accelerated during the transition from the LGM to interglacial conditions, yet only a few global estimates based on observations and modeling are available for the Quaternary. The bank, shelf, and slope carbonate sinks are still poorly constrained, but recent efforts have demonstrated the potential for modeling of neritic carbonate burial to fill the observational gaps.

5. ONGOING CHALLENGES AND OPPORTUNITIES

Despite the advances described in the preceding sections, our quantitative grasp of global glacial/interglacial carbonate burial remains limited. Significant uncertainties persist even for estimates of modern export, dissolution, and burial fluxes (e.g., Battaglia et al. 2016; Sulpis et al. 2021, 2022). A robust quantitative understanding of present-day carbonate burial is necessary if we expect to accurately estimate burial fluxes in the past and compare across glacial/interglacial cycles. We require greater attention to carbonate production, export, and preservation in marginal

environments, where our observations are sparse, yet we expect sea level–driven variations in burial over the glacial/interglacial cycles. On a global scale, proxies that are incorporated into carbonate and recorded in marine sediments, such as strontium and calcium isotopes, provide new opportunities to generate continuous records reflecting carbonate burial through time.

5.1. Heterogeneous Neritic Carbonate Sinks

As noted throughout this review, the complex mosaic of habitats on carbonate shelves, platforms, and reefs is a primary complication in estimating total carbonate production and sedimentation. In addition to corals, shallow marine organisms such as echinoderms (Lebrato et al. 2010), *Halimeda* algae (Drew 1983), and calcifiers living in seagrass ecosystems (Mazarrasa et al. 2015) produce significant amounts of neritic carbonate sediment, but their inclusion in global carbonate budgets has been limited. To better represent the contributions of these groups, we need new methods for characterizing their distribution and abundance. Since carbonate sedimentation by these calcifying organisms varies by species and habitat (e.g., Castro-Sanguino et al. 2020; de Macêdo Carneiro & de Morais 2016; de Macêdo Carneiro et al. 2018; Mazarrasa et al. 2015; Perry et al. 2017, 2019), the coverage of habitat type must be known in addition to within-habitat species abundance and sedimentation rates. Provided that there are adequate field-based estimates of the latter, satellite imagery might be leveraged to define habitat coverage (e.g., Perry et al. 2019, Utami et al. 2018) to scale localized studies to regional carbonate budgets for the modern shallow ocean.

5.2. *Halimeda* Bioherms

Recent studies of the *Halimeda* bioherms of the Great Barrier Reef demonstrated that this component of the Holocene neritic carbonate budget has been vastly underestimated. The bioherms—mounds of accumulated *Halimeda* skeletal fragments—record accumulation of *Halimeda* carbonate in some regions (for detailed descriptions of *Halimeda* bioherms, see Davies 2011, McNeil et al. 2020). New mapping with airborne lidar and multibeam bathymetry revealed that the Great Barrier Reef bioherms covered three times the previously estimated area (McNeil et al. 2016). With carbonate volumes equal to or greater than the adjacent coral reefs (Rees et al. 2006), these bioherms contributed significantly more to the shelf carbonate budget than has been accounted for (Iglesias-Rodriguez et al. 2002, Milliman 1993). Comparable volumes of carbonate were mapped on a carbonate platform off northwestern India (Rao et al. 2018). Globally extrapolating Great Barrier Reef *Halimeda* accumulation yields an estimated increase of ∼4–8% in the Holocene carbonate budget (Hinestrosa et al. 2022).

Other identified (but inadequately mapped) regions of Holocene bioherms include Kalukalukuang Bank in the eastern Java Sea, the Nicaraguan Rise in the southwest Caribbean, and the Big Bank Shoals in the Timor Sea (McNeil et al. 2020). Older fossil bioherms have been found on the Fifty Fathom Flat, India (Late Quaternary); Funafuti, Tuvalu (Pleistocene); the Solomon Islands (Pleistocene); and Vanuatu (Pliocene to Pleistocene) and have been studied little since their discoveries (McNeil et al. 2020). Estimates of the carbonate inventories of these bioherms, which will require updated mapping and analyses of carbonate content, can improve our estimates of how much carbonate was buried on shelves and platforms when these were flooded during interglacial periods.

5.3. Geochemical Proxies

Given the challenges of estimating global carbonate burial from direct observations, we can turn to geochemical proxies that reflect a global signal of the integrated carbonate fluxes. The precipitation of carbonate incorporates not only calcium (Ca^{2+}) but also trace amounts of magnesium

(Mg^{2+}) and strontium (Sr^{2+}) into the crystal structure. The effect of carbonate burial on the global ocean inventories of these elements and their isotopes, which in some cases are fractionated between seawater and precipitating carbonate, is recorded in the elemental ratios and isotopic composition of marine sediments. While magnesium isotope records indicate that carbonate deposition is not a primary control on seawater magnesium over the Cenozoic (Gothmann et al. 2017, Higgins & Schrag 2015), seawater Sr/Ca ratios (Stoll & Schrag 1998), strontium isotopes (Paytan et al. 2021), and calcium isotopes (Fantle 2010, Griffith & Fantle 2020) may be sensitive to glacial/interglacial variations in carbonate burial and thus serve as useful global proxies.

5.3.1. Strontium/calcium ratio. Strontium is added to the ocean by continental weathering and hydrothermal activity and removed by the precipitation of both neritic aragonite (strontium rich) and pelagic calcite (strontium poor). Due to the enrichment of strontium in aragonite ($D_{Sr} \approx 1$ for aragonite, compared with $D_{Sr} \approx 0.1$ for calcite), the ocean strontium inventory is strongly influenced by the burial of shelf aragonite, with a smaller effect from the partitioning of carbonate burial between the shallow and deep ocean (Graham et al. 1982, Schlanger 1988, Stoll & Schrag 1998). During glacial periods, sea level regression exposed continental shelves where metastable aragonite recrystallized to calcite and released large amounts of strontium to the ocean that were only partially reprecipitated in calcite. Such a change in seawater strontium concentrations would theoretically be reflected in the Sr/Ca ratio of seawater, as calcium is conserved during aragonite recrystallization, though concurrent variation in calcium fluxes could mute the change in the strontium/calcium ratio (Stoll & Schrag 1998).

Stoll & Schrag (1998) modeled a 1–3% change in seawater Sr/Ca over glacial/interglacial cycles, but direct reconstructions using planktic and benthic foraminifera yielded differing records with greater variability (Martin et al. 1999, Stoll et al. 1999). Reconstructing seawater Sr/Ca is an ongoing challenge, as illustrated by conflicting records of Cenozoic seawater Sr/Ca derived from gastropods, $CaCO_3$ veins, benthic foraminifera, fish teeth, corals, and belemnites/rudists (Balter et al. 2011, Coggon et al. 2010, Ivany et al. 2004, Lear et al. 2003, Sosdian et al. 2012, Steuber & Veizer 2002, Tripati et al. 2009). Such reconstructions are complicated by secondary effects such as growth rate, selective dissolution, and carbonate ion saturation, which influence carbonate Sr/Ca ratios to varying degrees depending on species (Elderfield et al. 2000, Stoll et al. 1999, Tripati et al. 2009, Yu et al. 2014). Furthermore, Lebrato et al. (2020) demonstrated significant global variability in modern seawater Sr/Ca ratios and suggested that regional environmental effects contributed to the differences among paleo seawater Sr/Ca records. Marine barite has been proposed as an alternative archive of seawater Sr/Ca (Averyt & Paytan 2003), as barite is not subject to the same biological effects as biogenic carbonate, but the potential influence of other factors (e.g., water depth) on barite strontium content has not been fully explored (Griffith & Paytan 2012). Despite these limitations, records of seawater strontium concentrations should not be discounted as a means of inferring carbonate burial rates. Among the next steps is further investigation of archives such as marine barite that may passively record seawater chemistry without biological or preservation effects.

5.3.2. Stable strontium isotopes. The stable strontium isotopic composition of seawater ($\delta^{88/86}Sr$) provides a new constraint on the ocean strontium budget (in addition to the traditional radiogenic strontium isotope ratio, $^{87}Sr/^{86}Sr$) (Krabbenhöft et al. 2010, Paytan et al. 2021, Pearce et al. 2015, Vollstaedt et al. 2014). Due to the fractionation of stable strontium isotopes between seawater and carbonate (−0.18‰) and the enrichment of strontium in aragonite, seawater $\delta^{88/86}Sr$ is sensitive to neritic carbonate burial and recrystallization. Paytan et al. (2021) published a seawater $\delta^{88/86}Sr$ record derived from marine barite over the past 35 My, demonstrating that $\delta^{88/86}Sr$

can be used to estimate variations in the ocean strontium inventory and infer changes in neritic carbonate burial. Significant variability in Quaternary seawater $\delta^{88/86}$Sr values suggests that the effect of glacial/interglacial shifts in shallow marine carbonate burial may be resolved with a high-resolution record (Paytan et al. 2021).

5.3.3. Stable calcium isotopes. Calcium isotopes also provide new insight, though their application to reconstructing past carbonate burial is not straightforward. Weathering is the primary input of calcium to the ocean, while $CaCO_3$ sedimentation removes calcium with a large fractionation of δ^{44}Ca (approximately −1.3‰) between seawater and $CaCO_3$ (Griffith & Fantle 2020). Though imbalances between the weathering and carbonate burial fluxes would theoretically be reflected by changes in seawater δ^{44}Ca, there is uncertainty around the assumption of a constant seawater-carbonate fractionation factor through time and the fidelity of calcium isotope archives (for an in-depth review of calcium isotopes and their application to the global calcium cycle, see Griffith & Fantle 2020). As future work resolves these issues, reconstructions of seawater calcium isotopes may prove useful for inferring carbonate burial changes.

5.4. Non-Steady-State Modeling

The potentially dynamic cycles of strontium and calcium in the ocean (e.g., Griffith et al. 2008, Paytan et al. 2021, Vance et al. 2009) can be modeled using the additional budget constraints provided by the geochemical proxies discussed above. Despite the long residence times of calcium (∼1 My) and strontium (∼2.5 My), extreme changes in weathering or carbonate sedimentation can drive budget imbalances over shorter timescales (e.g., glacial/interglacial cycles). There is little evidence that the decrease in neritic carbonate burial during glacial periods was compensated for by an increase in deep-sea burial. Deglacial changes in weathering regimes and weatherability are also possible (Vance et al. 2009). If we relax the assumption that the ocean strontium and calcium cycles were at steady state over the Quaternary, changes in the $\delta^{88/86}$Sr and δ^{44}Ca of seawater may reflect transient imbalances in the weathering and carbonate burial fluxes (e.g., Griffith et al. 2008, Krabbenhöft et al. 2010, Paytan et al. 2021, De La Rocha & DePaolo 2000, Vollstaedt et al. 2014). Though using these isotopic records to obtain continuous records of past global carbonate burial will require robust constraints on input fluxes and isotopic composition, this is a promising approach for quantifying Quaternary carbonate burial.

6. CONCLUSIONS

Significant advances in quantifying present-day and Quaternary carbonate burial have been made over the last few decades. Compilations of deep-sea carbonate accumulation records yielded improved global flux estimates for the Holocene and LGM. Various modeling approaches have been used to better quantify burial fluxes in shallow marine environments. Increasing recognition of underestimated components of the neritic carbonate budget has prompted investigations of carbonate accumulation by *Halimeda* algae, echinoderms, and other shallow-ocean dwellers that must be incorporated into future carbonate budgets.

Nevertheless, accurate reconstruction of global carbonate burial over glacial/interglacial timescales remains challenging, largely due to the difficulty of obtaining a continuous global record from discrete observations. Continued exploration of glacial-age carbonate fluxes throughout the deep sea will help evaluate hypotheses related to the geographic variations in carbonate burial. Emerging paleoceanographic proxies such as the stable strontium and calcium isotope systems can also help fill these gaps.

The links between marine carbonate burial and atmospheric pCO_2 via the ocean carbonate system prompted the idea that sea level–driven shifts in carbonate burial had an impact on Quaternary

climate, potentially accounting for ~6–20 ppm of the observed ~90-ppm pCO_2 rise recorded in ice cores from the LGM to Holocene (Kohfeld & Ridgwell 2009, Ridgwell et al. 2003). The magnitude and consequences of this mechanism may only be fully explored when we have confidently quantified the global carbonate burial fluxes in the shallow and deep ocean over glacial/interglacial cycles.

DISCLOSURE STATEMENT

The authors are not aware of any affiliations, memberships, funding, or financial holdings that might be perceived as affecting the objectivity of this review.

ACKNOWLEDGMENTS

We are grateful to J. Zachos and the reviewer for insightful and constructive comments that improved this review. We also thank Production Editor J. Duncan for rigorous editing of the manuscript.

LITERATURE CITED

Anderson RF, Fleisher MQ, Lao Y, Winckler G. 2008. Modern $CaCO_3$ preservation in equatorial Pacific sediments in the context of late-Pleistocene glacial cycles. *Mar. Chem.* 111:30–46

Andersson AJ. 2014. The oceanic $CaCO_3$ cycle. In *Treatise on Geochemistry*, ed. HD Holland, KK Turekian, pp. 519–42. Oxford: Elsevier. 2nd ed.

Archer DE. 1991. Equatorial Pacific calcite preservation cycles: production or dissolution? *Paleoceanography* 6:561–71

Archer DE. 2010. *The Global Carbon Cycle*. Princeton, NJ: Princeton Univ. Press

Archer DE, Maier-Reimer E. 1994. Effect of deep-sea sedimentary calcite preservation on atmospheric CO_2 concentration. *Nature* 367:260–63

Armstrong McKay D. 2015. *Investigating the drivers of perturbations to the Cenozoic carbon-climate system*. PhD Thesis, Univ. Southampton, Southampton, UK

Arrhenius G. 1952. *Sediment Cores from the East Pacific*. Rep. Swed. Deep-Sea Exped. 1947–1948 Vol. 5. Göteburg, Swed.: Elanders

Averyt KB, Paytan A. 2003. Empirical partition coefficients for Sr and Ca in marine barite: implications for reconstructing seawater Sr and Ca concentrations. *Geochem. Geophys. Geosyst.* 4:1039

Balsam WL. 1983. Carbonate dissolution on the Muir Seamount (western North Atlantic); interglacial/glacial changes. *J. Sediment. Res.* 53:719–31

Balsam WL, McCoy FW Jr. 1987. Atlantic sediments: glacial/interglacial comparisons. *Paleoceanography* 2:531–42

Balter V, Lécuyer C, Barrat J-A. 2011. Reconstructing seawater Sr/Ca during the last 70 My using fossil fish tooth enamel. *Palaeogeogr. Palaeoclimatol. Palaeoecol.* 310:133–38

Bassinot FC, Beaufort L, Vincent E, Labeyrie LD, Rostek F, et al. 1994. Coarse fraction fluctuations in pelagic carbonate sediments from the tropical Indian Ocean: a 1500-kyr record of carbonate dissolution. *Paleoceanography* 9:579–600

Battaglia G, Steinacher M, Joos F. 2016. A probabilistic assessment of calcium carbonate export and dissolution in the modern ocean. *Biogeosciences* 13:2823–48

Berger WH. 1982. Increase of carbon dioxide in the atmosphere during deglaciation: the coral reef hypothesis. *Naturwissenschaften* 69:87–88

Berner RA. 2003. The long-term carbon cycle, fossil fuels and atmospheric composition. *Nature* 426:323–26

Berner RA. 2004. *The Phanerozoic Carbon Cycle: CO_2 and O_2*. Oxford, UK: Oxford Univ. Press

Biscaye PE, Kolla V, Turekian KK. 1976. Distribution of calcium carbonate in surface sediments of the Atlantic Ocean. *J. Geophys. Res.* 81:2595–603

Boudreau BP, Luo Y. 2017. Retrodiction of secular variations in deep-sea $CaCO_3$ burial during the Cenozoic. *Earth Planet. Sci. Lett.* 474:1–12

Broecker WS. 2003. The oceanic $CaCO_3$ cycle. In *Treatise on Geochemistry*, ed. HD Holland, KK Turekian, pp. 529–49. Oxford, UK: Pergamon. 1st ed.

Broecker WS. 2009. Wally's quest to understand the ocean's $CaCO_3$ cycle. *Annu. Rev. Mar. Sci.* 1:1–18

Broecker WS, Peng T-H. 1982. *Tracers in the Sea*. New York: Eldigio

Broecker WS, Peng T-H. 1987. The role of $CaCO_3$ compensation in the glacial to interglacial atmospheric CO_2 change. *Glob. Biogeochem. Cycles* 1:15–29

Brovkin V, Ganopolski A, Archer D, Rahmstorf S. 2007. Lowering of glacial atmospheric CO_2 in response to changes in oceanic circulation and marine biogeochemistry. *Paleoceanography* 22:PA4202

Cabioch G, Montaggioni L, Thouveny N, Frank N, Sato T, et al. 2008. The chronology and structure of the western New Caledonian barrier reef tracts. *Palaeogeogr. Palaeoclimatol. Palaeoecol.* 268:91–105

Camoin GF, Ebren P, Eisenhauer A, Bard E, Faure G. 2001. A 300 000-yr coral reef record of sea level changes, Mururoa atoll (Tuamotu archipelago, French Polynesia). *Palaeogeogr. Palaeoclimatol. Palaeoecol.* 175:325–41

Camoin GF, Seard C, Deschamps P, Webster JM, Abbey E, et al. 2012. Reef response to sea-level and environmental changes during the last deglaciation: Integrated Ocean Drilling Program Expedition 310, Tahiti Sea Level. *Geology* 40:643–46

Camoin GF, Webster JM. 2015. Coral reef response to Quaternary sea-level and environmental changes: state of the science. *Sedimentology* 62:401–28

Campbell SM, Moucha R, Derry LA, Raymo ME. 2018. Effects of dynamic topography on the Cenozoic carbonate compensation depth. *Geochem. Geophys. Geosyst.* 19:1025–34

Cartapanis O, Galbraith ED, Bianchi D, Jaccard SL. 2018. Carbon burial in deep-sea sediment and implications for oceanic inventories of carbon and alkalinity over the last glacial cycle. *Clim. Past* 14:1819–50

Castro-Sanguino C, Bozec Y-M, Mumby PJ. 2020. Dynamics of carbonate sediment production by Halimeda: implications for reef carbonate budgets. *Mar. Ecol. Prog. Ser.* 639:91–106

Catubig NR, Archer DE, Francois R, deMenocal P, Howard W, Yu E-F. 1998. Global deep-sea burial rate of calcium carbonate during the Last Glacial Maximum. *Paleoceanography* 13:298–310

Clark PU, McCabe AM, Mix AC, Weaver AJ. 2004. Rapid rise of sea level 19,000 years ago and its global implications. *Science* 304:1141–44

Coggon RM, Teagle DAH, Smith-Duque CE, Alt JC, Cooper MJ. 2010. Reconstructing past seawater Mg/Ca and Sr/Ca from mid-ocean ridge flank calcium carbonate veins. *Science* 327:1114–17

Costa KM, Hayes CT, Anderson RF, Pavia FJ, Bausch A, et al. 2020. ^{230}Th normalization: new insights on an essential tool for quantifying sedimentary fluxes in the modern and Quaternary ocean. *Paleoceanogr. Paleoclimatol.* 35:e2019PA003820

Crowley TJ. 1985. Late Quaternary carbonate changes in the North Atlantic and Atlantic/Pacific comparisons. In *The Carbon Cycle and Atmospheric CO2: Natural Variations Archean to Present*, ed. WS Broecker, ET Sundquist, pp. 271–84. Washington, DC: Am. Geophys. Union

Davies PJ. 2011. Halimeda bioherms. In *Encyclopedia of Modern Coral Reefs: Structure, Form and Process*, ed. D Hopley, pp. 535–49. Dordrecht, Neth.: Springer

de Macêdo Carneiro PB, de Morais JO. 2016. Carbonate sediment production in the equatorial continental shelf of South America: quantifying *Halimeda incrassata* (Chlorophyta) contributions. *J. S. Am. Earth Sci.* 72:1–6

de Macêdo Carneiro PB, Pereira JU, Matthews-Cascon H. 2018. Standing stock variations, growth and $CaCO_3$ production by the calcareous green alga *Halimeda opuntia*. *J. Mar. Biol. Assoc. UK* 98:401–9

De La Rocha CL, DePaolo DJ. 2000. Isotopic evidence for variations in the marine calcium cycle over the Cenozoic. *Science* 289:1176–78

deMenocal P, Archer D, Leth P. 1997. Pleistocene variations in deep Atlantic circulation and calcite burial between 1.2 and 0.6 Ma: a combined data-model approach. In *Proceedings of the Ocean Drilling Program: Scientific Results*, Vol. 154: *Ceara Rise*, ed. NJ Shackleton, WB Curry, C Richter, TJ Bralower, pp. 285–98. College Station, TX: Ocean Drill. Program

Drew EA. 1983. Halimeda biomass, growth rates and sediment generation on reefs in the central great barrier reef province. *Coral Reefs* 2:101–10

Dullo W-C. 2005. Coral growth and reef growth: a brief review. *Facies* 51:33–48

Dunne JP, Hales B, Toggweiler JR. 2012. Global calcite cycling constrained by sediment preservation controls. *Glob. Biogeochem. Cycles* 26:GB3023

Elderfield H, Cooper M, Ganssen G. 2000. Sr/Ca in multiple species of planktonic foraminifera: implications for reconstructions of seawater Sr/Ca. *Geochem. Geophys. Geosyst.* 1:1017

Fairbanks RG. 1989. A 17,000-year glacio-eustatic sea level record: influence of glacial melting rates on the Younger Dryas event and deep-ocean circulation. *Nature* 342:637–42

Fantle MS. 2010. Evaluating the Ca isotope proxy. *Am. J. Sci.* 310:194–230

Farrell JW, Prell WL. 1989. Climatic change and $CaCO_3$ preservation: an 800,000 year bathymetric Reconstruction from the central equatorial Pacific Ocean. *Paleoceanography* 4:447–66

Francois R, Frank M, Rutgers van der Loeff MM, Bacon MP. 2004. ^{230}Th normalization: an essential tool for interpreting sedimentary fluxes during the late Quaternary. *Paleoceanography* 19:PA1018

Frank TD, James NP, Bone Y, Malcolm I, Bobak LE. 2014. Late Quaternary carbonate deposition at the bottom of the world. *Sediment. Geol.* 305:1–16

Fu H, Jian X, Zhang W, Shang F. 2020. A comparative study of methods for determining carbonate content in marine and terrestrial sediments. *Mar. Pet. Geol.* 116:104337

Gothmann AM, Stolarski J, Adkins JF, Higgins JA. 2017. A Cenozoic record of seawater Mg isotopes in well-preserved fossil corals. *Geology* 45:1039–42

Graham D, Bender M, Williams DF, Keigwin L. 1982. Strontium-calcium ratios in Cenozoic planktonic foraminifera. *Geochim. Cosmochim. Acta* 46:1281–92

Greene SE, Ridgwell A, Kirtland Turner S, Schmidt DN, Pälike H, et al. 2019. Early Cenozoic decoupling of climate and carbonate compensation depth trends. *Paleoceanogr. Paleoclimatol.* 34:930–45

Griffith EM, Fantle MS. 2020. *Calcium Isotopes*. Cambridge, UK: Cambridge Univ. Press

Griffith EM, Paytan A. 2012. Barite in the ocean – occurrence, geochemistry and palaeoceanographic applications. *Sedimentology* 59:1817–35

Griffith EM, Paytan A, Caldeira K, Bullen TD, Thomas E. 2008. A dynamic marine calcium cycle during the past 28 million years. *Science* 322:1671–74

Hain M, Sigman D, Haug G. 2014. The biological pump in the past. In *Treatise on Geochemistry*, ed. HD Holland, KK Turekian, pp. 485–517. Oxford: Elsevier. 2nd ed.

Hayes CT, Costa KM, Anderson RF, Calvo E, Chase Z, et al. 2021. Global ocean sediment composition and burial flux in the deep sea. *Glob. Biogeochem. Cycles* 35:e2020GB006769

Hebbeln D, Bender M, Gaide S, Titschack J, Vandorpe T, et al. 2019. Thousands of cold-water coral mounds along the Moroccan Atlantic continental margin: distribution and morphometry. *Mar. Geol.* 411:51–61

Higgins JA, Schrag DP. 2015. The Mg isotopic composition of Cenozoic seawater – evidence for a link between Mg-clays, seawater Mg/Ca, and climate. *Earth Planet. Sci. Lett.* 416:73–81

Hinestrosa G, Webster JM, Beaman RJ. 2022. New constraints on the postglacial shallow-water carbonate accumulation in the Great Barrier Reef. *Sci. Rep.* 12:924

Husson L, Pastier A-M, Pedoja K, Elliot M, Paillard D, et al. 2018. Reef carbonate productivity during Quaternary sea level oscillations. *Geochem. Geophys. Geosyst.* 19:1148–64

Iglesias-Rodriguez MD, Armstrong R, Feely R, Hood R, Kleypas J, et al. 2002. Progress made in study of ocean's calcium carbonate budget. *Eos Trans. AGU* 83:365–75

Isson TT, Planavsky NJ, Coogan LA, Stewart EM, Ague JJ, et al. 2020. Evolution of the global carbon cycle and climate regulation on Earth. *Glob. Biogeochem. Cycles* 34:e2018GB006061

Ivany LC, Peters SC, Wilkinson BH, Lohmann KC, Reimer BA. 2004. Composition of the early Oligocene ocean from coral stable isotope and elemental chemistry. *Geobiology* 2:97–106

Jaccard SL, Galbraith ED, Sigman DM, Haug GH, Francois R, et al. 2009. Subarctic Pacific evidence for a glacial deepening of the oceanic respired carbon pool. *Earth Planet. Sci. Lett.* 277:156–65

Jones NS, Ridgwell A, Hendy EJ. 2015. Evaluation of coral reef carbonate production models at a global scale. *Biogeosciences* 12:1339–56

Jorry S, Jouet G, Edinger EN, Toucanne S, Counts JW, et al. 2020. From platform top to adjacent deep sea: new source-to-sink insights into carbonate sediment production and transfer in the SW Indian Ocean 2 (Glorieuses archipelago). *Mar. Geol.* 423:106144

Kastens KA, Mascle J, Auroux C, Bonatti E, Broglia C, et al., eds. 1987. *Proceedings of the Ocean Drilling Program: Initial Report*, Vol. 107: *Tyrrhenian Sea Sites 650–656*. College Station, TX: Ocean Drill. Program

Kerr J, Rickaby R, Yu J, Elderfield H, Sadekov AY. 2017. The effect of ocean alkalinity and carbon transfer on deep-sea carbonate ion concentration during the past five glacial cycles. *Earth Planet. Sci. Lett.* 471:42–53

Kleypas JA. 1997. Modeled estimates of global reef habitat and carbonate production since the Last Glacial Maximum. *Paleoceanography* 12:533–45

Kleypas JA, Anthony KRN, Gattuso J-P. 2011. Coral reefs modify their seawater carbon chemistry – case study from a barrier reef (Moorea, French Polynesia). *Glob. Change Biol.* 17:3667–78

Kohfeld KE, Ridgwell A. 2009. Glacial-interglacial variability in atmospheric CO_2. In *Surface Ocean: Lower Atmosphere Processes*, ed. C Le Quéré, ES Saltzman, pp. 251–86. Washington, DC: Am. Geophys. Union

Krabbenhöft A, Eisenhauer A, Böhm F, Vollstaedt H, Fietzke J, et al. 2010. Constraining the marine strontium budget with natural strontium isotope fractionations ($^{87}Sr/^{86}Sr^*$, $\delta^{88/86}Sr$) of carbonates, hydrothermal solutions and river waters. *Geochim. Cosmochim. Acta* 74:4097–109

Laugié M, Michel J, Pohl A, Poli E, Borgomano J. 2019. Global distribution of modern shallow-water marine carbonate factories: a spatial model based on environmental parameters. *Sci. Rep.* 9:16432

Lear CH, Elderfield H, Wilson PA. 2003. A Cenozoic seawater Sr/Ca record from benthic foraminiferal calcite and its application in determining global weathering fluxes. *Earth Planet. Sci. Lett.* 208:69–84

Lebrato M, Garbe-Schönberg D, Müller MN, Blanco-Ameijeiras S, Feely RA, et al. 2020. Global variability in seawater Mg:Ca and Sr:Ca ratios in the modern ocean. *PNAS* 117:22281–92

Lebrato M, Iglesias-Rodríguez D, Feely RA, Greeley D, Jones DOB, et al. 2010. Global contribution of echinoderms to the marine carbon cycle: $CaCO_3$ budget and benthic compartments. *Ecol. Monogr.* 80:441–67

Lindberg B, Mienert J. 2005. Postglacial carbonate production by cold-water corals on the Norwegian Shelf and their role in the global carbonate budget. *Geology* 33:537–40

Lough JM. 2008. Coral calcification from skeletal records revisited. *Mar. Ecol. Prog. Ser.* 373:257–64

Lyle M. 2003. Neogene carbonate burial in the Pacific Ocean. *Paleoceanography* 18:1059

Lyle M, Barron J, Bralower TJ, Huber M, Lyle AO, et al. 2008. Pacific Ocean and Cenozoic evolution of climate. *Rev. Geophys.* 46:RG2002

Lyle M, Drury AJ, Tian J, Wilkens R, Westerhold T. 2019. Late Miocene to Holocene high-resolution eastern equatorial Pacific carbonate records: stratigraphy linked by dissolution and paleoproductivity. *Clim. Past* 15:1715–39

Lyle M, Olivarez A, Backman J, Tripati A. 2006. Biogenic sedimentation in the Eocene equatorial Pacific—the stuttering greenhouse and Eocene carbonate compensation depth. In *Proceedings of the Ocean Drilling Program: Scientific Results*, Vol. 199: *Paleogene Equatorial Transect Sites 1215–1222*, ed. PA Wilson, M Lyle, JV Firth. College Station, TX: Ocean Drill. Program. **https://doi.org/10.2973/odp.proc.sr.199.219.2005**

Martin PA, Lea DW, Mashiotta TA, Papenfuss T, Sarnthein M. 1999. Variation of foraminiferal Sr/Ca over Quaternary glacial-interglacial cycles: evidence for changes in mean ocean Sr/Ca? *Geochem. Geophys. Geosyst.* 1:1004

Mazarrasa I, Marbà N, Lovelock CE, Serrano O, Lavery PS, et al. 2015. Seagrass meadows as a globally significant carbonate reservoir. *Biogeosciences* 12:4993–5003

McGee D, Marcantonio F, McManus JF, Winckler G. 2010. The response of excess ^{230}Th and extraterrestrial ^{3}He to sediment redistribution at the Blake Ridge, western North Atlantic. *Earth Planet. Sci. Lett.* 299:138–49

McNeil MA, Nothdurft LD, Dyriw NJ, Webster JM, Beaman RJ. 2020. Morphotype differentiation in the Great Barrier Reef *Halimeda* bioherm carbonate factory: internal architecture and surface geomorphometrics. *Depos. Rec.* 7:176–99

McNeil MA, Webster JM, Beaman RJ, Graham TL. 2016. New constraints on the spatial distribution and morphology of the *Halimeda* bioherms of the Great Barrier Reef, Australia. *Coral Reefs* 35:1343–55

Milliman JD. 1993. Production and accumulation of calcium carbonate in the ocean: budget of a nonsteady state. *Glob. Biogeochem. Cycles* 7:927–57

Milliman JD, Droxler AW. 1996. Neritic and pelagic carbonate sedimentation in the marine environment: Ignorance is not bliss. *Geol. Rundsch.* 85:496–504

Montaggioni LF, Cabioch G, Thouveny N, Frank N, Sato T, Sémah A-M. 2011. Revisiting the Quaternary development history of the western New Caledonian shelf system: from ramp to barrier reef. *Mar. Geol.* 280:57–75

Mörth C-M, Backman J. 2011. Practical steps for improved estimates of calcium carbonate concentrations in deep sea sediments using coulometry. *Limnol. Oceanogr. Methods* 9:565–70

O'Mara NA, Dunne JP. 2019. Hot spots of carbon and alkalinity cycling in the coastal oceans. *Sci. Rep.* 9:4434

Opdyke BN, Walker JCG. 1992. Return of the coral reef hypothesis: basin to shelf partitioning of $CaCO_3$ and its effect on atmospheric CO_2. *Geology* 20:733–36

Pälike H, Lyle M, Nishi H, Raffi I, Ridgwell A, et al. 2012. A Cenozoic record of the equatorial Pacific carbonate compensation depth. *Nature* 488:609–14

Paytan A, Griffith EM, Eisenhauer A, Hain MP, Wallmann K, Ridgwell A. 2021. A 35-million-year record of seawater stable Sr isotopes reveals a fluctuating global carbon cycle. *Science* 371:1346–50

Pearce CR, Parkinson IJ, Gaillardet J, Charlier BLA, Mokadem F, Burton KW. 2015. Reassessing the stable ($\delta^{88/86}Sr$) and radiogenic ($^{87}Sr/^{86}Sr$) strontium isotopic composition of marine inputs. *Geochim. Cosmochim. Acta* 157:125–46

Perry CT, Morgan KM, Yarlett RT. 2017. Reef habitat type and spatial extent as interacting controls on platform-scale carbonate budgets. *Front. Mar. Sci.* 4:185

Perry CT, Salter MA, Morgan KM, Harborne AR. 2019. Census estimates of algal and epiphytic carbonate production highlight tropical seagrass meadows as sediment production hotspots. *Front. Mar. Sci.* 6:120

Rao VP, Mahale VP, Chakraborty B. 2018. Bathymetry and sediments on the carbonate platform off western India: significance of *Halimeda* bioherms in carbonate sedimentation. *J. Earth Syst. Sci.* 127:106

Rees SA, Opdyke BN, Wilson PA, Henstock TJ. 2006. Significance of *Halimeda* bioherms to the global carbonate budget based on a geological sediment budget for the Northern Great Barrier Reef, Australia. *Coral Reefs* 26:177–88

Rickaby REM, Elderfield H, Roberts N, Hillenbrand C-D, Mackensen A. 2010. Evidence for elevated alkalinity in the glacial Southern Ocean. *Paleoceanography* 25:1209

Ridgwell A, Watson AJ, Maslin MA, Kaplan JO. 2003. Implications of coral reef buildup for the controls on atmospheric CO_2 since the Last Glacial Maximum. *Paleoceanography* 18:1083

Ridgwell A, Zeebe R. 2005. The role of the global carbonate cycle in the regulation and evolution of the Earth system. *Earth Planet. Sci. Lett.* 234:299–315

Ryan DA, Opdyke BN, Jell JS. 2001. Holocene sediments of Wistari Reef: towards a global quantification of coral reef related neritic sedimentation in the Holocene. *Palaeogeogr. Palaeoclimatol. Palaeoecol.* 175:173–84

Schlager W, Reijmer JJG, Droxler A. 1994. Highstand shedding of carbonate platforms. *J. Sediment. Res.* 64:270–81

Schlanger SO. 1988. Strontium storage and release during deposition and diagenesis of marine carbonates related to sea-level variations. In *Physical and Chemical Weathering in Geochemical Cycles*, ed. A Lerman, M Meybeck, pp. 323–39. Dordrecht, Neth.: Springer

Sigman DM, Boyle EA. 2000. Glacial/interglacial variations in atmospheric carbon dioxide. *Nature* 407:859–69

Silverman J, Lazar B, Cao L, Caldeira K, Erez J. 2009. Coral reefs may start dissolving when atmospheric CO_2 doubles. *Geophys. Res. Lett.* 36:L05606

Silverman J, Lazar B, Erez J. 2007. Effect of aragonite saturation, temperature, and nutrients on the community calcification rate of a coral reef. *J. Geophys. Res. Oceans* 112:C05004

Smith S, Mackenzie F. 2016. The role of $CaCO_3$ reactions in the contemporary oceanic CO_2 cycle. *Aquat. Geochem.* 22:153–75

Sosdian SM, Lear CH, Tao K, Grossman EL, O'Dea A, Rosenthal Y. 2012. Cenozoic seawater Sr/Ca evolution. *Geochem. Geophys. Geosyst.* 13:Q10014

Steuber T, Veizer J. 2002. Phanerozoic record of plate tectonic control of seawater chemistry and carbonate sedimentation. *Geology* 30:1123–26

Stoll HM, Schrag DP. 1998. Effects of Quaternary sea level cycles on strontium in seawater. *Geochim. Cosmochim. Acta* 62:1107–18

Stoll HM, Schrag DP, Clemens SC. 1999. Are seawater Sr/Ca variations preserved in quaternary foraminifera? *Geochim. Cosmochim. Acta* 63:3535–47

Sulpis O, Agrawal P, Wolthers M, Munhoven G, Walker M, Middelburg J. 2022. Aragonite dissolution protects calcite at the seafloor. *Nat. Commun.* 13:1104

Sulpis O, Jeansson E, Dinauer A, Lauvset SK, Middelburg JJ. 2021. Calcium carbonate dissolution patterns in the ocean. *Nat. Geosci.* 14:423–28

Sundquist ET, Visser K. 2003. The geologic history of the carbon cycle. In *Treatise on Geochemistry*, ed. HD Holland, KK Turekian, pp. 425–72. Oxford, UK: Pergamon. 1st ed.

Titschack J, Baum D, De Pol-Holz R, Lopez Correa M, Forster N, et al. 2015. Aggradation and carbonate accumulation of Holocene Norwegian cold-water coral reefs. *Sedimentology* 62:1873–98

Titschack J, Fink HG, Baum D, Wienberg C, Hebbeln D, Freiwald A. 2016. Mediterranean cold-water corals – an important regional carbonate factory? *Depos. Rec.* 2:74–96

Tripati AK, Allmon WD, Sampson DE. 2009. Possible evidence for a large decrease in seawater strontium/calcium ratios and strontium concentrations during the Cenozoic. *Earth Planet. Sci. Lett.* 282:122–30

Utami DA, Reuning L, Cahyarini SY. 2018. Satellite- and field-based facies mapping of isolated carbonate platforms from the Kepulauan Seribu Complex, Indonesia. *Depos. Rec.* 4:255–73

Van Andel TH. 1975. Mesozoic/Cenozoic calcite compensation depth and the global distribution of calcareous sediments. *Earth Planet. Sci. Lett.* 26:187–94

Van Andel TH, Heath GR, Moore TC. 1975. Cenozoic history and paleoceanography of the central equatorial Pacific Ocean: a regional synthesis of Deep Sea Drilling Project data. Boulder, CO: Geol. Soc. Am.

van der Ploeg R, Boudreau BP, Middelburg JJ, Sluijs A. 2019. Cenozoic carbonate burial along continental margins. *Geology* 47:1025–28

Vance D, Teagle DAH, Foster GL. 2009. Variable Quaternary chemical weathering fluxes and imbalances in marine geochemical budgets. *Nature* 458:493–96

Vanden Berg MDV, Jarrard RD. 2002. Determination of equatorial Pacific mineralogy using light absorption spectroscopy. In *Proceedings of the Ocean Drilling Program: Initial Report*, Vol. 199: *Paleogene Equatorial Transect Sites 1215–1222*, ed. M Lyle, PA Wilson, TR Janecek, J Backman, WH Busch, et al. College Station, TX: Ocean Drill. Program. **https://doi.org/10.2973/odp.proc.ir.199.105.2002**

Vanden Berg MDV, Jarrard RD. 2004. Cenozoic mass accumulation rates in the equatorial Pacific based on high-resolution mineralogy of Ocean Drilling Program Leg 199. *Paleoceanography* 19:A2021

Vanden Berg MDV, Jarrard RD. 2006. Data report: high-resolution mineralogy for Leg 199 based on reflectance spectroscopy and physical properties. In *Proceedings of the Ocean Drilling Program: Scientific Results*, Vol. 199: *Paleogene Equatorial Transect Sites 1215–1222*, ed. PA Wilson, M Lyle, JV Firth. College Station, TX: Ocean Drill. Program. **https://doi.org/10.2973/odp.proc.sr.199.203.2006**

Vecsei A. 2004a. Carbonate production on isolated banks since 20 k.a. BP: climatic implications. *Palaeogeogr. Palaeoclimatol. Palaeoecol.* 214:3–10

Vecsei A. 2004b. A new estimate of global reefal carbonate production including the fore-reefs. *Glob. Planet. Change* 43:1–18

Vecsei A, Berger WH. 2004. Increase of atmospheric CO_2 during deglaciation: constraints on the coral reef hypothesis from patterns of deposition. *Glob. Biogeochem. Cycles* 18:GB1035

Vollstaedt H, Eisenhauer A, Wallmann K, Boehm F, Fietzke J, et al. 2014. The Phanerozoic $\delta^{88/86}$Sr record of seawater: new constraints on past changes in oceanic carbonate fluxes. *Geochim. Cosmochim. Acta* 128:249–65

Walker JCG, Opdyke BC. 1995. Influence of variable rates of neritic carbonate deposition on atmospheric carbon dioxide and pelagic sediments. *Paleoceanography* 10:415–27

Wallmann K, Aloisi G. 2012. The global carbon cycle: geological processes. In *Fundamentals of Geobiology*, ed. AH Knoll, DE Canfield, KO Konhauser, pp. 20–35. Chichester, UK: Wiley-Blackwell

Webster JM, Braga JC, Humblet M, Potts DC, Iryu Y, et al. 2018. Response of the Great Barrier Reef to sea-level and environmental changes over the past 30,000 years. *Nat. Geosci.* 11:426–32

Yokoyama Y, Esat TM, Thompson WG, Thomas AL, Webster JM, et al. 2018. Rapid glaciation and a two-step sea level plunge into the Last Glacial Maximum. *Nature* 559:603–7

Yu J, Elderfield H, Jin Z, Tomascak P, Rohling EJ. 2014. Controls on Sr/Ca in benthic foraminifera and implications for seawater Sr/Ca during the late Pleistocene. *Quat. Sci. Rev.* 98:1–6

Yu J, Menviel L, Jin ZD, Anderson RF, Jian Z, et al. 2020. Last glacial atmospheric CO_2 decline due to widespread Pacific deep-water expansion. *Nat. Geosci.* 13:628–33

Zeebe RE. 2012. History of seawater carbonate chemistry, atmospheric CO_2, and ocean acidification. *Annu. Rev. Earth Planet. Sci.* 40:141–65

Zeebe RE, Marchitto TM. 2010. Atmosphere and ocean chemistry. *Nat. Geosci.* 3:386–87

Zeebe RE, Westbroek P. 2003. A simple model for the $CaCO_3$ saturation state of the ocean: the "Strangelove," the "Neritan," and the "Cretan" Ocean. *Geochem. Geophys. Geosyst.* 4:1104